DUPLICATE

Forecasting Development

Forecasting Research Technical Report No. 390

Development of a short range QPF algorithm based upon Optic Flow Techniques

By N. Bowler and C.E. Pierce

May 2002

© Crown Copyright 2002

Met Office , NWP Division , Room 344, London Road , Bracknell , Berkshire ,RG12 2SZ, United Kingdom

00/0486

Forecasting Research
Technical Report No. 390

Development of a short range QPF algorithm based upon Optic Flow techniques

By

Neill Bowler and Clive Pierce

May 2002

Met Office
Joint Centre for Hydro-Meteorological Research
Maclean Building
Crowmarsh Gifford
Wallingford
Oxfordshire
OX10 8BB
United Kingdom

© Crown Copyright 2002

Permission to quote from this paper should be obtained from the above Met Office division

Executive summary

A new rain advection based nowcast scheme has been developed for Gandolf. This uses optic flow ideas [Horn & Schunck, 1981] to improve forecasting skill. The method employed removes the need to split the radar derived rain analysis into contiguous rain areas, but uses a smoothness constraint to ensure that the diagnosed velocity field varies smoothly across the analysis. The scheme has been shown to improve nowcasts of precipitation associated with cyclonic circulation around low pressure areas, and has also demonstrated superior performance during cases of embedded convection.

Optic flow methods derive from a direct application of the Optic Flow Constraint (OFC) equation. The terms in this equation are evaluated over a square block, which is considered to move with a single velocity. This velocity is found using a least squares method (see [Bab-Hadiashar & Suter, 1998]). Block velocities are smoothed, and an instantaneous rain rate forecast is produced.

The performance of the new nowcast scheme has been compared with that of the existing Gandolf advection scheme (not including the object-oriented conceptual life cycle model). The performance of the two schemes was compared over a period of 3 months. The new scheme showed a general improvement in forecast skill, and also demonstrated superior performance on a number of key test cases, including two precipitation events associated with severe flooding. On the basis of this evaluation, it is recommended that the optic flow scheme replace the existing Gandolf advection scheme.

A completely new approach to precipitation nowcasting has been developed. This affords numerous avenues for further research and development. These include the tuning of model parameters, the possibility of using 5-minute rain analyses, and moving to a continuous data assimilation framework. However, future advances in deterministic precipitation nowcasting are likely to come from modelling the evolution of rain intensity.

1 Motivation

1.1 Introduction & Background

Precipitation has long been one of the most difficult aspects of weather to forecast (see, for example [NWP index] reference). Over the last two decades operational weather radar networks have provided a quantitative means of establishing the spatial distribution of rainfall in near real time. This information has underpinned the development of various Quantitative Precipitation Forecast (QPF) algorithms based on extrapolation of current observations [Wilson *et al.*, 1998]. The perishability of the resultant QPFs is a reflection of both the simplicity of the extrapolation techniques employed, and the evolutionary complexity of rainfall patterns.

Gandolf is an automated system for generating short range (0 to 3 hour) forecasts of precipitation with high spatial (2 km) and temporal (5 minute) resolutions[1]. Its principle purpose is to improve QPFs over small river catchments prone to flash flooding caused by heavy rain [Pierce *et al.*, 2000]. Currently, precipitation forecasts from Numerical Weather Prediction (NWP) sources are of insufficient accuracy and resolution for quantitative fluvial flood prediction. In the short term, this state of affairs is likely to persist, hence the importance of improving algorithms that rely upon the extrapolation of processed radar data.

Two QPF schemes lie at the heart of the Gandolf system. An advection scheme similar to that implemented in Nimrod is used to forecast stratiform precipitation and showers associated with non-severe convection. For those relatively rare (<10 per year) cases of severe convection, a convective life model simulates multi-cell storm propagation by daughter cell generation [Hand, 1996; Pierce and Cooper, 2000].

The current Gandolf system has several known flaws. In particular, concern has been raised about the treatment of areas of intense precipitation embedded within stratiform rain areas. These relatively small scale features often exhibit a different, apparent velocity to that of the larger rain areas. This problem can be generalised to one of recognising and quantifying differential motion in sequences of radar derived rain analyses. An idealised illustration of this is shown in figure 1.

[1] There are plans to extend the temporal range of Gandolf forecasts to T+6 hours.

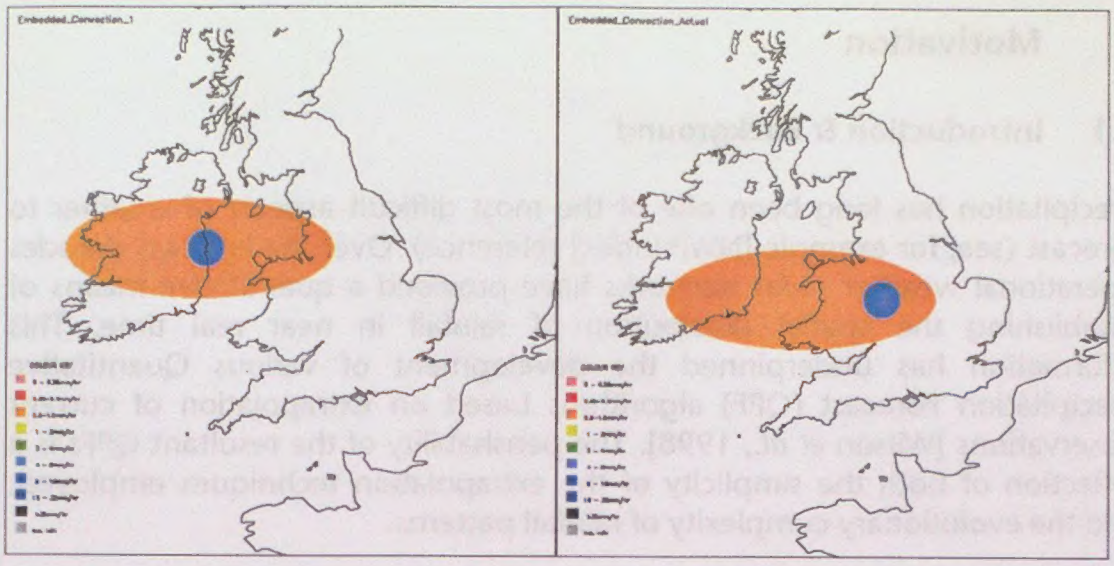

Figure 1. An idealised case of embedded convection. The large area of rain is moving eastwards more slowly than the intense "cell" embedded within it.

1.2 The current advection scheme in Gandolf

The advection scheme currently implemented in Gandolf was designed to be as similar as possible to that implemented in the 5 km Nimrod forecast scheme [Ryall, 1994]. The nowcasting approach adopted in Gandolf involves disaggregation of the radar observed precipitation field into distinct precipitation "objects" [Pierce & Cooper, 2000]. This is achieved by applying certain rules regarding the expected size of objects and the minimum separation distance between them. An optimal motion vector is determined for each object based upon its recently observed motion. Object position, size and assigned motion vector are stored in a file referred to as an "object details" file.

The advection scheme requires three initial inputs: the object details file from the previous hour's run (T-60 minutes), the rain analysis from the previous hour's run, and the current rain analysis. Precipitation identified in the current analysis is divided into objects according to the predefined limits on object separation distance and the total number of objects allowed. The latter is limited to ensure efficient and timely running of the analysis and forecast schemes. If the number of objects exceeds the specified limit, the objects closest to each other are combined until the total number is equal to, or lower than the limit.

Rain analyses from T-1 hour and T+0 are compared. This allows objects in analyses valid at T-1 hour and T+0 to be matched, and associated velocity vectors to be estimated. These vectors are used to determine whether a cross correlation vector or a meso-scale NWP model (the Met Office's Mesoscale Model, hereafter referred to as the MM) wind vector will best predict object motion in the recent past. An object details file for the current time is created. This contains skill scores comparing the performance of forecasts produced

using these two advection techniques. The most skilful method is used to forecast object motion. This may vary from object to object.

In an advection forecast sequence, objects and their associated segments [Ryall, 1994] initially form a seamless analysis. As objects follow their prescribed motion vectors, gaps will begin to appear between divergent segments. These gaps are filled using a time synchronous precipitation forecast from the MM. The latter can differ quite markedly from the true precipitation pattern and this combination can give rise to products of poor quality, both quantitatively and qualitatively.

From the perspective of handling scale dependent differential motion, the current advection scheme has significant limitations. The cross correlation extrapolator treats a rainfall object as a single, unchanging entity that moves with an assigned velocity. The MM wind advection algorithm allows objects to change shape and intensity, but not in accordance with radar observation. Rather, the objects are deformed, often unrealistically, by a field of MM wind vectors whose inferred extrapolations need not necessarily bear any direct relationship to observed rainfall movement.

2 Overview of the new forecast scheme

Current extrapolation forecasting methods fall into three broad categories – those that use correlation techniques [Hilst & Russo, 1960, Bellon & Austin, 1978], those that track the centroid of an object [Barclay & Wilk, 1970, Johnson et al, 1998], and those that use NWP wind advection techniques [Tatehira and Makino, 1974; Smith, 1975; Tatehira et al., 1976; Parsons and Hobbs, 1983]. Currently, the QPF scheme in Gandolf combines cross correlation and NWP based wind advection algorithms to forecast the motion of a discrete set of rain objects.

A slightly different approach involves the TREC (Tracking Radar Echoes by Correlation) method [Rinehart & Garvey, 1978]. Here, a rain analysis is arbitrarily split into a number of blocks in such a way that a Contiguous Rain Area (CRA) may be split over a number of blocks. The optimal advection vector for each block is determined using a correlation method. Thus, an area of rain may change shape, but gaps may be left where blocks diverge. The COTREC algorithm addresses this problem [Li *et al.*, 1995] by minimising the divergence of the velocities of adjacent blocks (that is minimising $\frac{\partial u}{\partial x}+\frac{\partial v}{\partial y}$). This criterion preserves precipitation area and eliminates spurious advection velocities caused by clutter and ground shielding.

The new extrapolation scheme, detailed below, is similar to the TREC method in that the velocity is calculated over pre-determined blocks. The velocity of each block is not calculated by correlation methods, but by direct application of the Optic Flow Constraint (OFC; see equation 1 below). A different

smoothness constraint to the COTREC approach is applied to the velocities of neighbouring blocks, but the spirit of the approach is similar. It is argued that the use of the OFC is superior to correlation methods, since it provides a natural framework for dealing with the growth and decay of precipitation areas. Figure 2 summarises the design and components of the scheme.

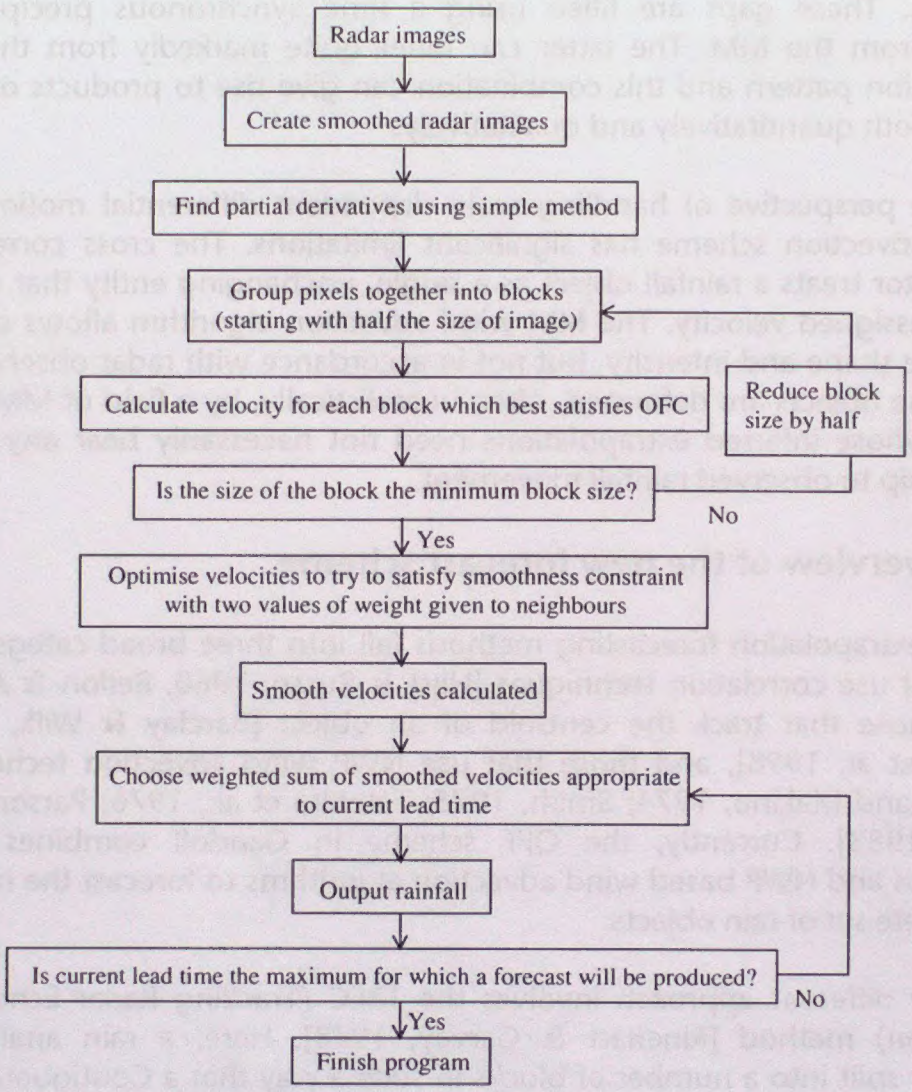

Figure 2. Schematic representation of the optic flow forecast scheme.

2.1 The Optic Flow Constraint (OFC)

Optic flow theory (also known as optical flow) has evolved for determining the motion of objects identified within an image [Horn & Schunck, 1981]. This is of particular interest in the field of computer vision, since robots need automated procedures for detecting motion. Such generalised approaches are of use in rainfall forecasting, and have been used in this area without knowledge of the optic flow literature [Laroche & Zawadzki, 1995].

Central to the study of optic flow is the Optic Flow Constraint equation (OFC). This makes explicit the assumption that features in an image sequence only change shape and do not change in size or intensity. For flow in two dimensions this is

$$D_t I = u\frac{\partial I}{\partial x} + v\frac{\partial I}{\partial y} + \frac{\partial I}{\partial t} = 0 \qquad (1)$$

where (u,v) is the velocity at each point in the images and $I(x,y)$ is the rainfall intensity. I is known at every point and an image sequence may be used to estimate the partial derivatives in equation (1). Thus, an expression relating u and v at every point may be found. The OFC may be visualised as constraining the flow velocity at every point to lie on a given line.

The OFC contains insufficient information to fully determine the flow velocity at every image pixel. Therefore, a number of techniques have been developed to provide this extra information [Bab-Hadiashar & Suter, 1998]. One such technique involves aggregating blocks of pixels (e.g. 10x10 pixels) and finding a single vector that best satisfies all the constraint lines given by the OFC for each block. Methods for establishing the best fit can vary from a least squares approach to a robust technique [Bab-Hadiashar & Suter, 1998] that is most appropriate in the presence of noise.

2.2 The continuity equation and smoothing of the velocity field

For many applications the most appropriate way to provide the extra information to solve the optic flow problem is to insist that the flow of the rainfall pattern is constrained by the continuity equation, which is given by

$$\nabla.(I\mathbf{V}) + \frac{\partial I}{\partial t} = 0 \qquad (2)$$

where $\mathbf{V} = (u,v)$. Upon substitution of the OFC this simplifies to

$$\nabla.\mathbf{V} = 0 \qquad (3)$$

where it is assumed that I is non-negative everywhere, and positive somewhere. Equations 1 and 2 combine to require divergence-free flow. This is the condition satisfied in the COTREC scheme [Li *et al.*, 1995].

In a similar vein, the following condition insists that the flow be smooth by minimising $\nabla^2\mathbf{V}$. Expanding $\nabla^2\mathbf{V}$ into its component parts it is seen that this is equivalent to minimising $\frac{\partial^2 u}{\partial x^2} + \frac{\partial^2 u}{\partial y^2}$ and $\frac{\partial^2 v}{\partial x^2} + \frac{\partial^2 v}{\partial y^2}$. Performing a Taylor expansion to second order this term becomes

$$\left| u(x,y) - \frac{u(x+\delta,y)+u(x,y+\delta)+u(x-\delta,y)+u(x,y-\delta)}{4} \right|$$ and similarly for v.

Hence, minimising $\nabla^2\mathbf{V}$ is equivalent to minimising the difference between the velocity of each pixel/block and the average velocity of its neighbouring pixels/blocks. Minimising $\nabla^2\mathbf{V}$ is therefore described as a smoothness constraint.

2.3 Justification for choosing the OFC & smoothness constraint

One may object to the application of equation 1 and the smoothness constraint to the advection of rainfall on the grounds that neither will be strictly obeyed by an evolving rainfall pattern. The OFC assumes that rainfall objects remain constant in intensity, and only change in shape, but a shower cloud, for example, can develop and decay in a matter of minutes [Wilson *et al.*, 1998], and the fine structure of stratiform rain bands can be equally short lived. Furthermore, although the velocity field of a rainfall pattern often appears smooth, there is no reason why this should always be the case, or why the field should be smooth in the manner dictated by the smoothness constraint.

On the other hand, the assumption underlying the OFC is common in precipitation nowcasting and underpins the advection scheme in the current Gandolf system. The smoothness condition will provide velocity fields which appear realistic and should help to avoid spurious advection velocities. Both equations, although not strictly obeyed by rainfall, should produce sensible flow patterns that mimic the actual movement of rainfall well. Moreover, these conditions provide a natural framework for considering the growth and decay of rain areas.

3 Implementation details

Having introduced the topic of optic flow, and the underlying assumptions of the proposed forecast scheme, some of the finer details of the new scheme are discussed in the followed sub-sections.

3.1 Estimating the partial derivatives of the OFC equation

The typical maximum advection velocity of rainfall objects is approximately 130 km h^{-1} [Ulbrich *et al.*, 2001]. Hence, a rain object may move by as much as 33 km in the 15 minute interval between successive composite rain analyses[2], a distance equivalent to 16 pixels on a 2 km Cartesian grid. This velocity maximum implies that partial derivative estimates in the OFC must be reliable for objects moving at this rate or less.

[2] The UK weather radars perform a scan every 5 minutes, but the data from the radar network are merged into a single, composite analysis every 15 minutes.

There are well established, sophisticated techniques for partial derivative estimation: the Leapfrog and Runge-Kutta methods are good examples [O'Neil, 1995]. Some authors favour using the derivatives of a Gaussian function [Bab-Hadiashar & Suter, 1998]. The method chosen in the new forecast scheme is simpler. Consecutive composite rain analyses are smoothed, and the derivatives found using a local estimation method [Horn & Schunck, 1981]. This approach is fast, yet provides good estimates of the OFC derivatives for rainfall velocities as large as 100 km h^{-1}.

The smoothing mask is a square box centred on the pixel for which the average is to be taken. The smoothed intensity is given by

$$I_{\text{smoothed}}(x_0, y_0) = \frac{1}{(2L_s+1)^2} \sum_{x=x_0-L_s}^{x_0+L_s} \sum_{y=y_0-L_s}^{y_0+L_s} I(x, y), \qquad (4)$$

where $L_s = 7$. This choice of L_s implies that the smoothing occurs over a box of 15 by 15 pixels. Consequently, rainfall with a speed of more than 15 pixels per time step cannot be estimated accurately. Figure 3 shows that the velocity estimates of a 15 by 15 pixel box are accurate up to an actual velocity of 13 pixels per time step, or 104 km h^{-1} for rain analyses on a 2 km grid.

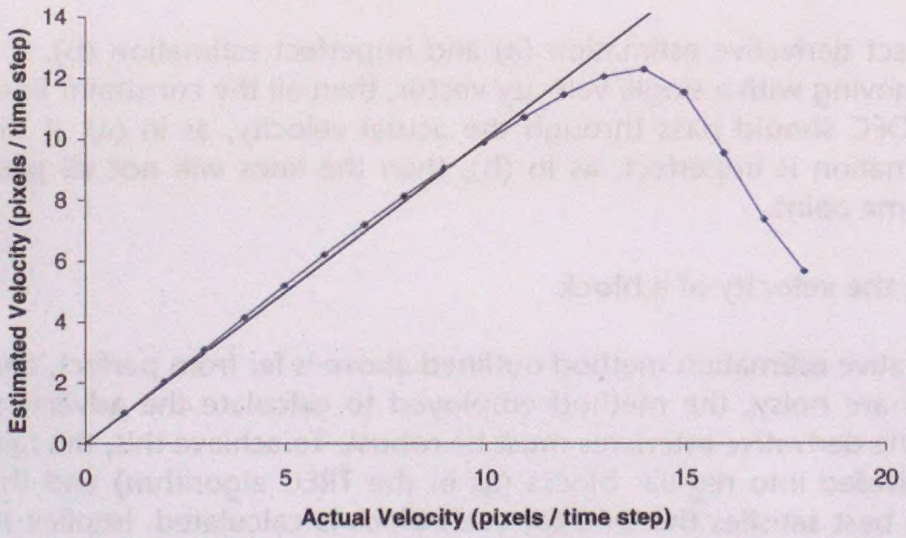

Figure 3. How the estimated velocity of a block varies with the actual velocity, using a smoothing mask with $L_s = 7$. The speed is well estimated for velocities less than 13 pixels per time step, but the speed tends to be under estimated as the actual velocity increases beyond 10 pixels per time step.

It might seem wise to choose a larger mask ($L_s > 7$) given that the mask size imposes an upper limit on the accurate estimation of block velocity. However, the larger the mask, the poorer the spatial resolution of the derivative estimates. Thus, the choice of L_s is a compromise between estimating large velocities with sufficient accuracy, and capturing the differential motion exhibited by neighbouring boxes.

The proposed method for estimating the OFC partial derivatives is far from perfect. Consider a scenario in which the entire precipitation field is moving with a fixed velocity (u,v). Estimating the partial derivatives at every pixel will give a set of simultaneous equations, each of which can be considered as constraining the velocity of that pixel to lie on a given line (see figure 4). If the derivative estimation is perfect, then all the lines will pass through the point (u,v), as shown in figure 4a. This cannot be expected from the method of derivative estimation outlined above. The situation will be closer to that illustrated in figure 4b.

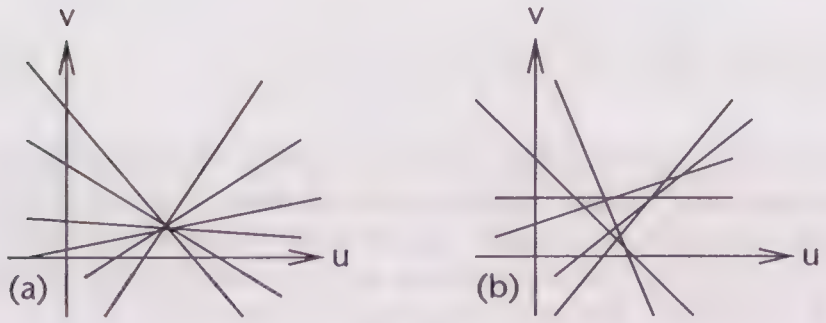

Figure 4. Perfect derivative estimation (a) and imperfect estimation (b). If a rain object is moving with a single velocity vector, then all the constraint lines given by the OFC should pass through the actual velocity, as in (a). If the derivative estimation is imperfect, as in (b), then the lines will not all pass through the same point.

3.2 Finding the velocity of a block

Since the derivative estimation method outlined above is far from perfect, and the radar data are noisy, the method employed to calculate the advection velocity from the derivative estimates must be robust. To achieve this, the rain analyses are divided into regular blocks (as in the TREC algorithm) and the velocity which best satisfies the OFC for each block is calculated. Implicit in this approach is the assumption that the actual velocity of rain within a block is constant.

The proposed method, however, allows blocks to overlap. Thus, the OFC may be used to compute a velocity for each pixel by finding the best solution to the OFC for a block centred on that pixel. In the new forecast scheme, the rain analysis is partitioned into 16x16 pixel blocks. The velocity of each of these blocks is found by solving the OFC on a 32x32 pixel block, centred on the 16x16 block. A least squares solution to the OFC has been adopted [Bab-Hadiashar & Suter, 1998]. This technique appears to produce similar results to those of more sophisticated algorithms, designed to cope with noisy data.

The choice of block size, in common with that of mask size, is a compromise between resolving rain motion at small scales and correctly representing the large scale structure of the velocity field. The OFC is solved for a series of block sizes ranging in horizontal dimensions from half the size of the rain analysis, down in factors of two, to the smallest block size, stated above. The velocity from the larger blocks is used to determine the velocity of smaller blocks where there is insufficient rain to solve the OFC. Gandolf rain analyses are currently 575^2 pixels, so the analysis was artificially extended with missing data to 1024^2 pixels ($1024=2^{10}$).

The velocities diagnosed at larger scales can be used to constrain the velocities at smaller scales. This is achieved by merging the velocities identified at the small and large scales according to

$$\mathbf{V}_{\text{small}}^{\text{merged}} = (1-r_h)\mathbf{V}_{\text{small}}^{\text{OFC}} + r_h\mathbf{V}_{\text{large}}^{\text{merged}}, \tag{5}$$

where r_h is a parameter to be chosen, and $\mathbf{V}_{\text{small}}^{\text{OFC}}$ refers to the solution of the OFC found at the smaller scale. The large scale velocities influence those at smaller scales through a cascade effect. This form of the cascade is useful since only one parameter is required. Figure 5 gives the RMSE for forecasts using varying values of the coefficient for the smoothness constraint, r_n, and for the weight given to the large scales, r_h. This suggests that the cascade is similar in effect to the smoothness constraint.

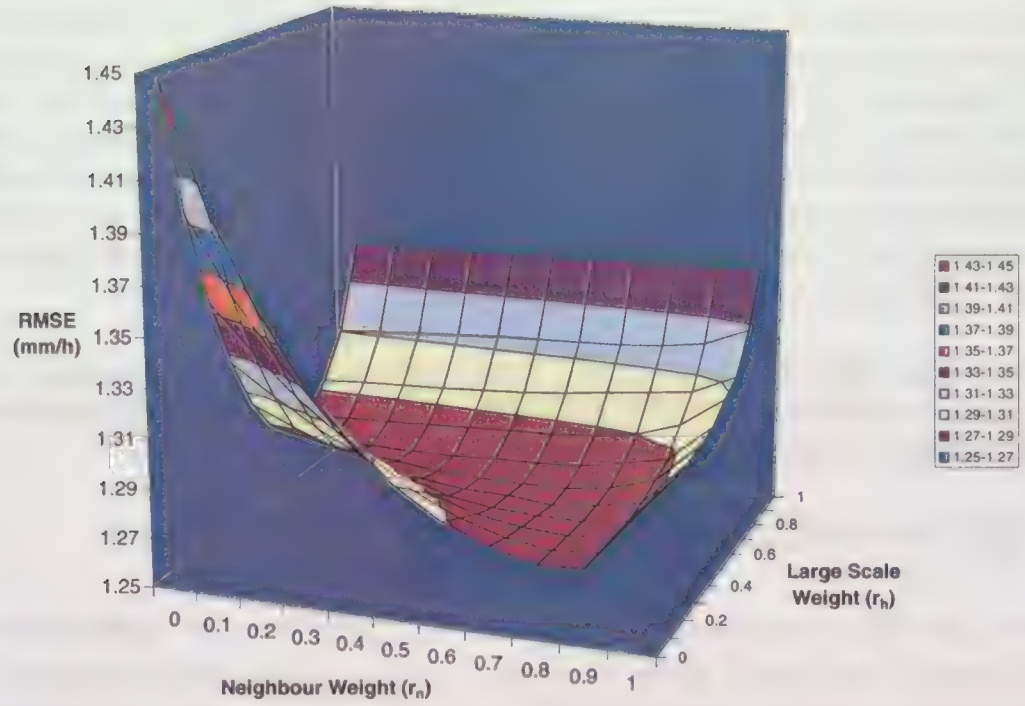

Figure 5. How the root mean square error (RMSE) of a 30 minute forecast (made at 0515 GMT on 23/1/2002) varies with the strength of the smoothness constraint, and the weight given to the velocity evaluated at larger scales (see equation 5). The evaluation of the smoothness constraint is explained in section 3.3.

3.3 Optimising the velocity field

After computation of the block velocities through application of the OFC, the new forecast scheme attempts to find the velocity field that best satisfies the smoothness constraint. This latter process is equivalent to demanding that the velocity of each block be equal to the average velocity of its neighbours. This would strictly mean finding the average of the 4 nearest neighbouring blocks, but better results are attained using the 8 nearest neighbours.

The first step in finding the velocity field which best satisfies the smoothness constraint involves calculating a weight for each block given by

$$K(x,y)=1-e^{-\frac{I_{av}(x,y)}{w}} \qquad (6)$$

where $I_{av}(x,y)$ is the average rain rate of the block located at (x,y), and $w>0$ is a parameter. This weight is applied such that no weight is given to blocks with zero total rain rate, but a block with an infinite rain rate would receive a weight of 1. w=3 mm h^{-1} was chosen, as this appeared to give good results. The weighted velocity is initially calculated as

$$\mathbf{V}_w(x,y) = K(x,y)\mathbf{V}_{OFC}(x,y), \qquad (7)$$

where $\mathbf{V}_{OFC}(x,y)$ is the best solution to the OFC for the block located at (x,y). This is used to calculate the weighted average velocity of the neighbouring blocks given by

$$\mathbf{V}_{neighbour}(x,y) = (\mathbf{V}_w(x+L,y) + \mathbf{V}_w(x-L,y) + \mathbf{V}_w(x,y+L) + \mathbf{V}_w(x,y-L))/6 + (\mathbf{V}_w(x+L,y+L) + \mathbf{V}_w(x+L,y-L) + \mathbf{V}_w(x-L,y+L) + \mathbf{V}_w(x-L,y-L))/12 \qquad (8)$$

where L is the size of each block. The velocity field that satisfies the smoothness constraint is found by calculating the following for every block:

$$\mathbf{V}'(x,y) = \left((1-r_n)K(x,y)\mathbf{V}_{OFC}(x,y) + r_n\mathbf{V}_{neighbour}(x,y)\right)/K_{total}(x,y) \qquad (9)$$

where $0<r_n<1$ is a parameter, and K_{total} is the average weight of the block and those of its neighbours. An iteration is performed for all blocks. $\mathbf{V}'$gives the new values of the velocity to replace $\mathbf{V}_{OFC}$ in equation (7), the latter being used to calculate $\mathbf{V}_w$. Twenty iterations of this scheme proved sufficient to allow the velocities to converge to a stable solution. This method for optimising the velocity field is robust and quick. A method based upon a global optimisation technique may be more robust, but would be much slower.

During the development and testing of the forecast scheme, the optimum values of r_n as a function of lead time were determined experimentally using case study data from January, 2002. Figure 6 compares the performance of the optic flow scheme as a function of the value of r_n used. It was found that smaller values of r_n were most appropriate for short lead times (0.95), whilst larger values were more appropriate for longer lead times (0.99). This is intuitive, because the large scale velocity is expected to be most important at longer lead times, and applying a bigger value of r_n gives more weight to the large scale motion.

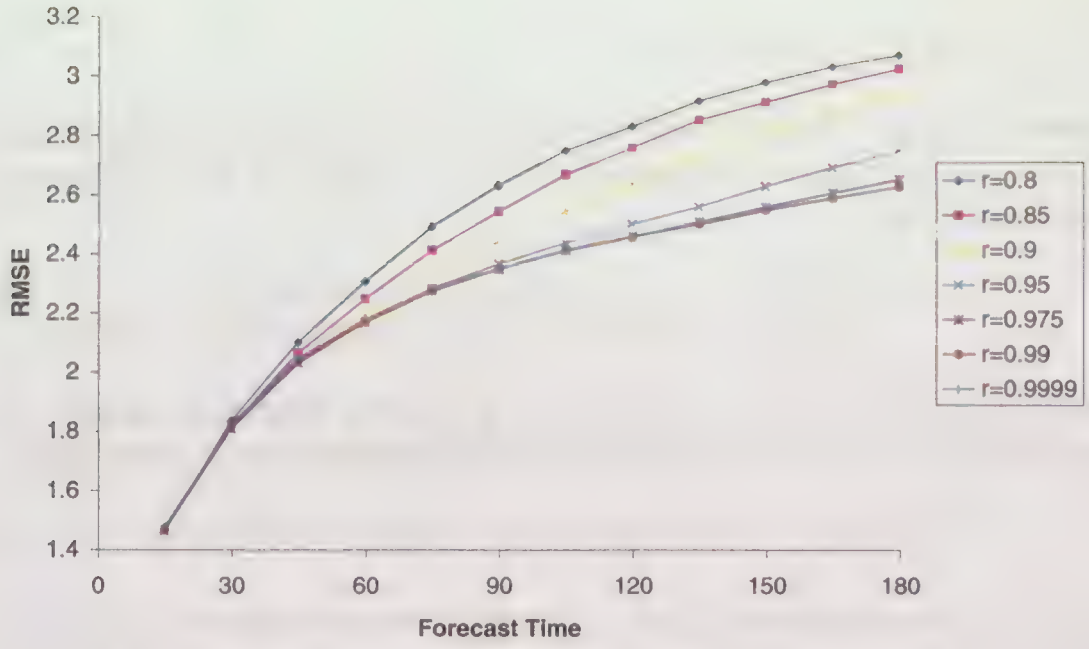

Figure 6. The RMS error of forecasts using varying values of r_n.

3.4 Choice of time interval between rain analysis pairs

The current Gandolf system ingests two rain analyses validating on consecutive hours, and finds which advection vectors best describe the observed transformations. The selection of a one hour time interval between analyses allows the motion of large rain areas to be captured, whilst minimising the effects of data digitisation. The choice of time interval remains to be fully addressed. It is likely to vary with forecast lead time, and the prevailing weather conditions (see figures 7a-b). A 15 minute time interval has been chosen in the absence of more detailed evidence. One might expect that a small time interval is best for short lead times, while a larger time interval is better for longer lead times.

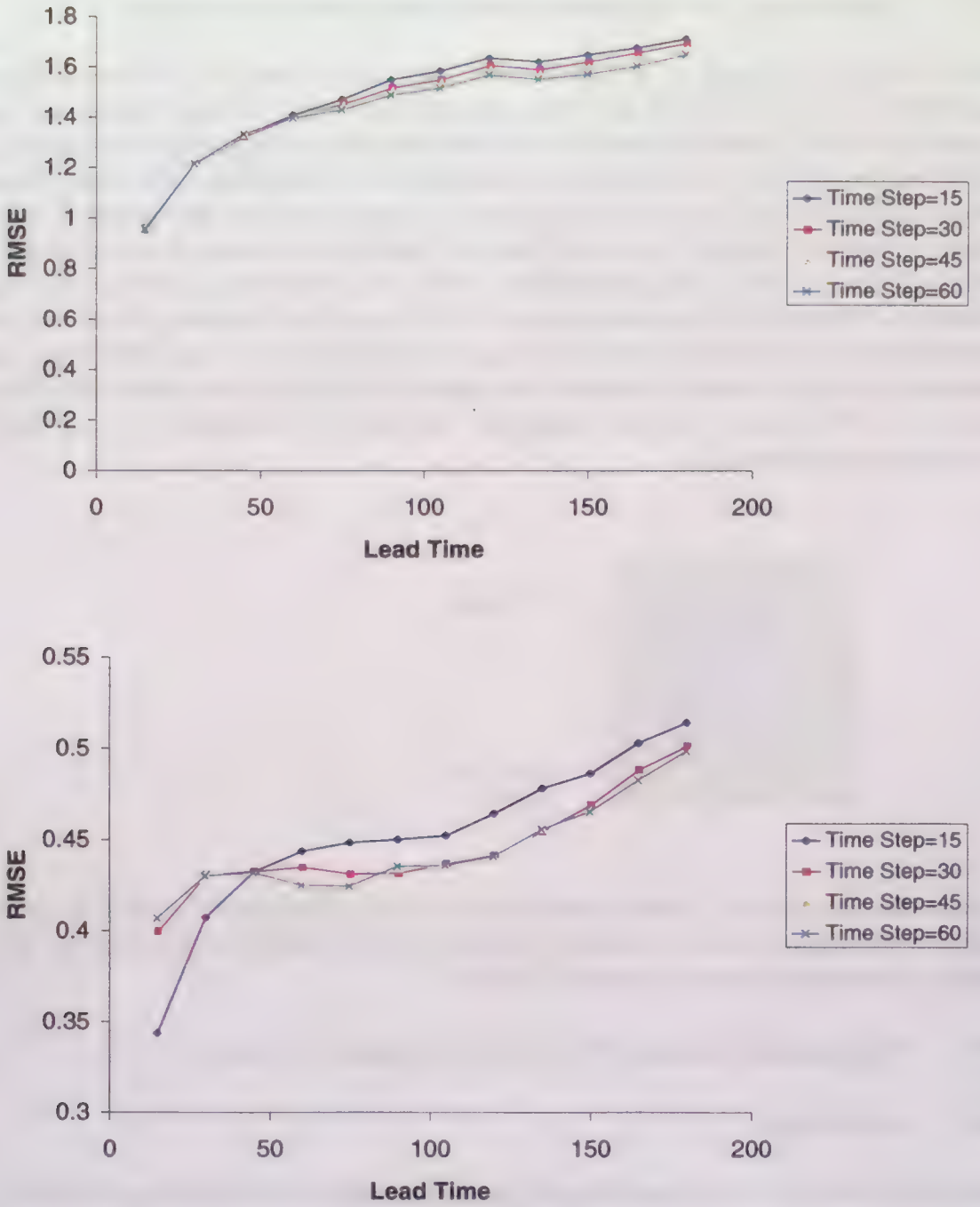

Figure 7. Investigation of the optimum choice of time interval between pairs of rain analyses. Plots of RMS forecast error are shown for a variety of different time intervals on two separate days. The optimum choice of time interval appears to vary with the prevailing weather conditions. (a) The average RMSE for forecasts using optic flow between 0345 GMT and 0515 GMT on 23 January 2002. (b) The average RMSE for forecasts using optic flow between 1130 GMT and 1300 GMT on 22 January 2002.

3.5 Distributing rainfall in an instantaneous rain rate forecast

The velocity assigned to a given pixel will, in general, be a non-integer number. Thus, a rain pixel will not normally "land on" a single pixel on the ground. Rather, it will be spread over four neighbouring pixels (see figure 8) in direct proportion to the area of coverage. In this manner rain from more than one rain pixel may be assigned to a single pixel on the ground. This implies that the forecast rain rate field will intensify in areas of convergence, but will be prone to fragmentation where neighbouring velocity vectors diverge. In the latter case, an example of the resultant banding effect in the predicted rain rate field is shown in figure 9 (bottom-left). This effect may be avoided by apportioning forecast rain evenly along the path taken by a rain pixel in the time interval between successive forecasts (i.e. a rain accumulation forecast).

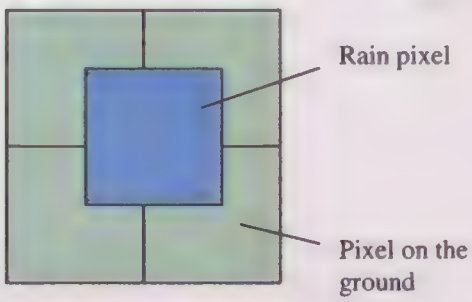

Figure 8. Assignment of the advected rain rate field to pixels on the ground. Rain in an advected pixel will be spread over four contiguous pixels on the ground in proportion to the area of overlap.

4 The performance of the new forecast scheme

4.1 Case Studies

A number of case studies are examined. Some of these relate to key historical rainfall events for which the existing Gandolf forecast scheme is known to have performed poorly. Others consider the performance of optic flow forecast scheme during a variety of rainfall events. These are included to demonstrate algorithm robustness.

4.1.1 Embedded Convection

Figure 1 shows an idealised case of embedded convection. The sharp boundaries between the high intensity feature and the low intensity feature mean that any inaccuracies in the forecast schemes will be evident immediately. Figure 9 compares the performance of a T+180 minute optic flow rain rate forecast with an equivalent Gandolf forecast. Figure 10 shows

the east-west component of the velocity diagnosed by the optic flow scheme through the centre of the feature.

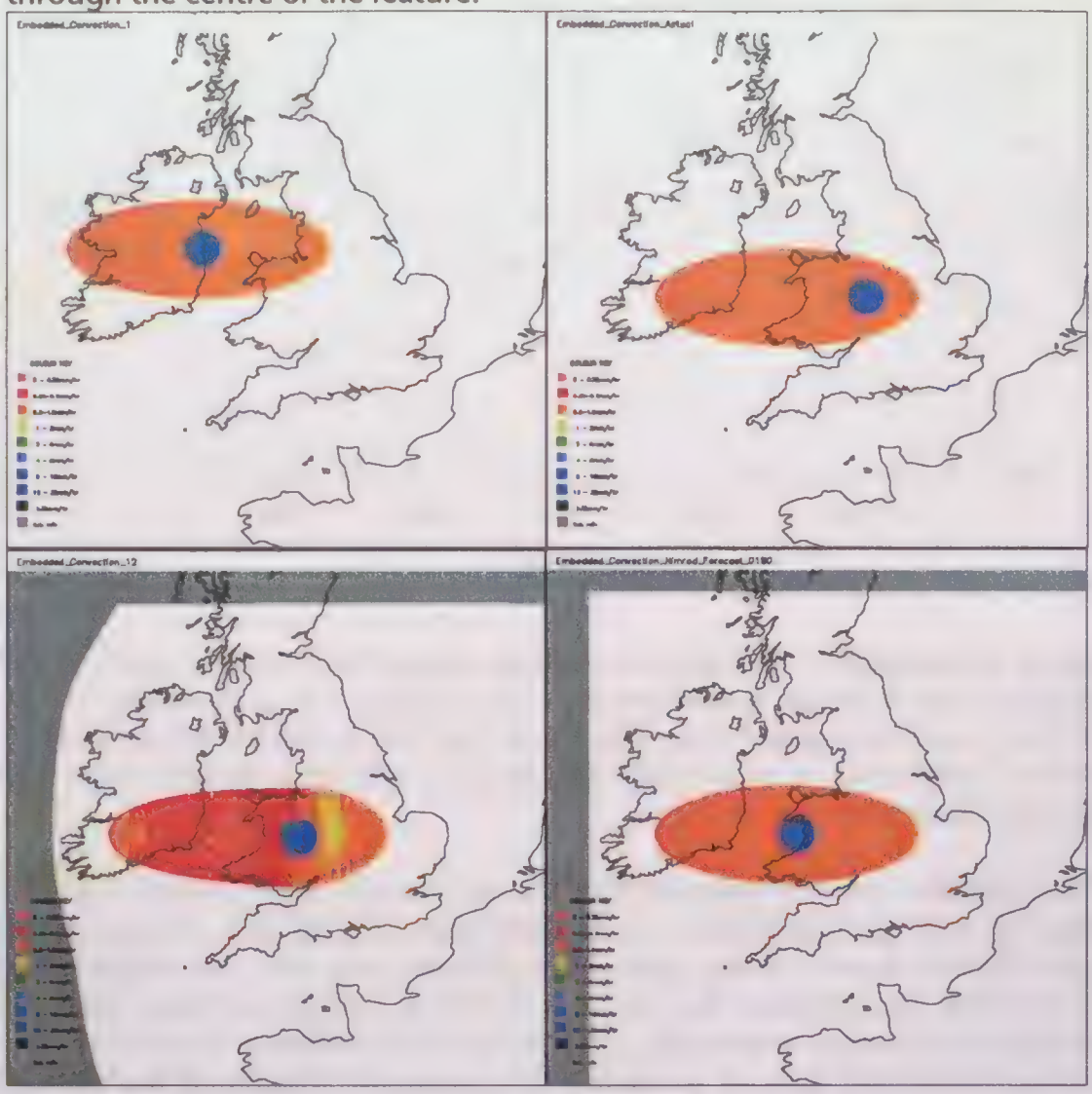

Figure 9. Comparison of T+180 minute optic flow and Gandolf rain rate forecasts for an artificial, embedded convection scenario, as shown in figure 1. The optic flow scheme (bottom-left) performs well in this case, capturing the relative motion of the precipitation band and its embedded high intensity feature with some skill. This is achieved by stretching the rain band either side of the intense precipitation core. The current Gandolf system (bottom-right) gets the motion of the larger area correct, but fails to account for the motion of the embedded feature.

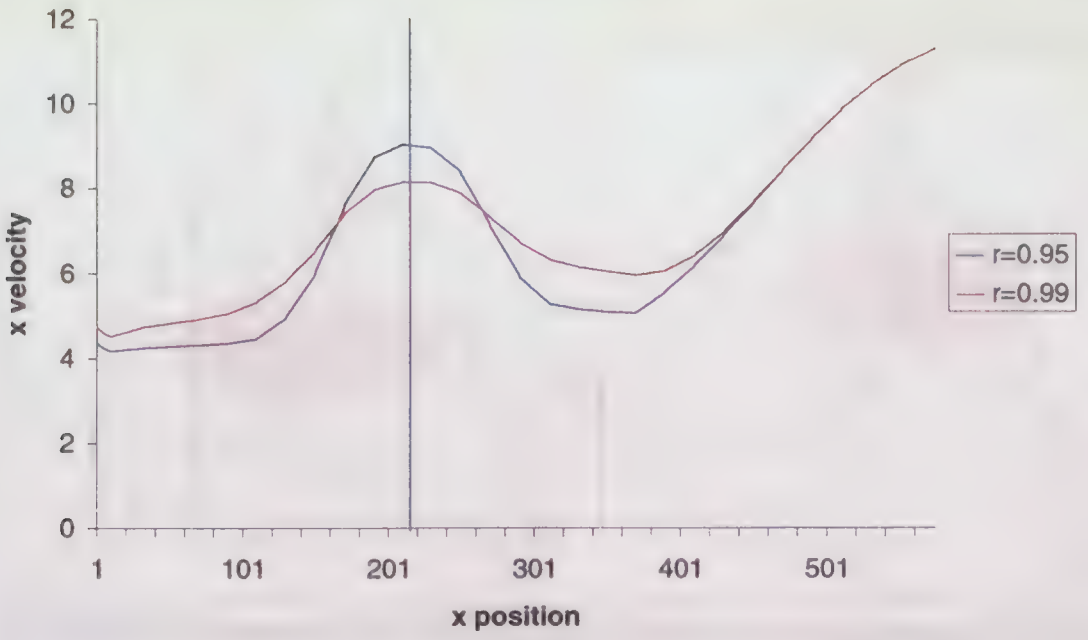

Figure 10. Variation in the east-west component of the forecast velocity in the idealised case of embedded convection. The velocity is accurate for the edges of the forecast rain area (marked by the orange lines), and for the embedded feature (marked by a blue line). The velocity is forced to vary smoothly between these points.

The optic flow scheme forecasts the idealised case of embedded convection relatively well compared with the Gandolf advection scheme. However, the high intensity feature is not advected sufficiently fast, and the stretching is undesirable. Nonetheless, the position of both the large rain area and the embedded feature is close to that observed at T+180 minutes. In contrast, the Gandolf advection forecast is unable to capture the motion of the intense precipitation core, but is reliable in its handling of the rain band as a whole.

4.1.2 9 April 1998

A deep low pressure system was centred off the coast of Cornwall. Associated fronts remained almost stationary over much of the Midlands and Wales. Several belts of precipitation oriented south-west to north-east contained embedded convection. This led to severe flooding in the Midlands with as much as 97mm of rain falling in 48 hours [Bye & Horner, 1998]. The near surface wind field demonstrated significant rotation about the low centre.

In this case study, the performance of the optic flow algorithm is compared with that of Nimrod, because suitable data were not available to run the equivalent Gandolf advection scheme. The comparison is justified because the Nimrod and Gandolf advection algorithms are almost identical.

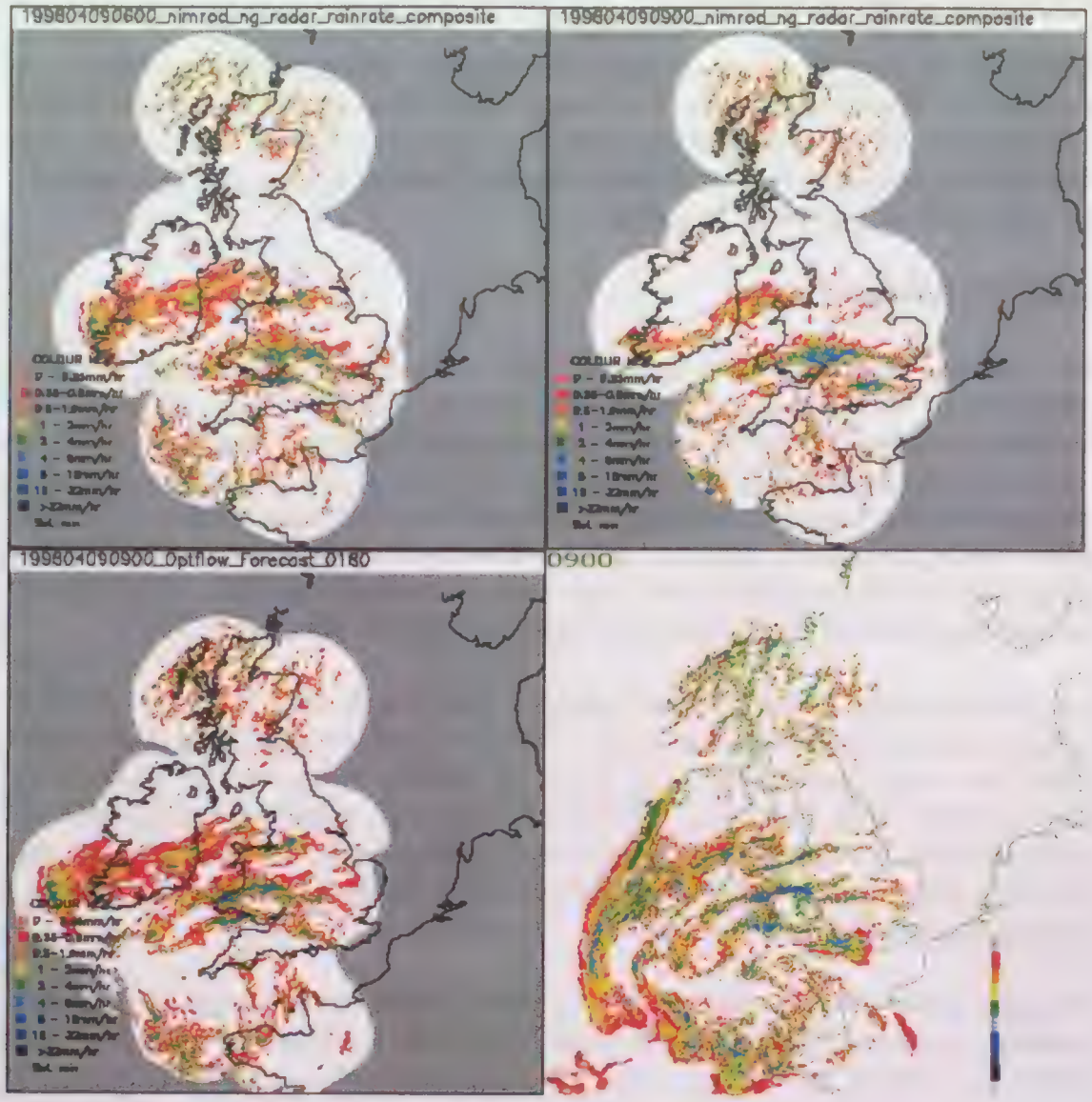

Figure 11. Verification of optic flow and Nimrod advection forecasts with a data time of 0600 GMT on 9 April 1998. The rain analyses valid at 0600 GMT (top-left) and 0900 GMT (top-right) should be compared with the T+3 hour forecasts from the optic flow (bottom-left) and Nimrod advection schemes (bottom-right).

The optic flow scheme predicts much of the rain over England and Wales to move gradually westwards (figure 11). This reflects the observed westward motion of the rain. In reasonable agreement with observation, the intense rainfall over the West Midlands and Wales remains almost stationary. The rotation observed in the precipitation field is captured.

By contrast, the Nimrod advection scheme moves the rain too quickly westwards with the result that predicted accumulations were significantly too low. The reason for this lies with the use of MM winds to perform the advection, since the wind speeds assigned to the rain objects were much too high. The fact that rainfall often moves with a different velocity to the wind field is well documented [Tatehira, 1976].

Although the forecast produced by the optic flow algorithm has its faults, it is a significant improvement on the Nimrod advection scheme because it better predicts the observed rainfall velocity. The stationary nature of the rain over Wales and the Midlands is difficult to capture because it is embedded within a broader scale feature moving quickly.

4.1.3 30 October 2000

An intense low-pressure system and associated widespread, heavy precipitation moved across the UK. Severe weather was widespread. Prolonged, heavy rain led to serious flooding, particularly in parts of northern England and Wales. A sequence of radar rain analyses for the day in question showed that the sustained rainfall in the north was associated with a relatively slow moving occlusion, wrapped around the centre of the depression. Further away from the depression centre, significant rotational motion was apparent in the broad band of frontal precipitation moving broadly west to east.

The performances of the Gandolf advection and optic flow forecast schemes are compared in figure 12. The majority of the Gandolf model runs moved the entire rain area eastwards using a single extrapolation vector (figure 12, bottom-right). This treatment failed to capture the rotational motion of the principle rain band, and the associated differences in translation velocity between the rapidly moving rain over southern England, and the slower moving precipitation in the north.

The optic flow scheme forecasts the motion with some measure of success, even the apparent rotation of the band originally over northern England and Wales. The higher translation velocity of the rain over southern England is handled satisfactorily. The most obvious deficiency of the forecast is the failure of the scheme to decay the rainfall associated with the tip of the wrap-around occlusion. This is beyond the capabilities of both optic flow and Gandolf advection algorithms.

A greater concern lies with the velocities assigned to areas close to the boundary of the image. There can be features near the boundary that are only present in one of the rain analyses, meaning $\left|\frac{\partial I}{\partial t}\right|$ will be large and the assigned velocity vector can also be large. This is seen from the irregular shape of the "no data" area in the south-west corner of the domain. Banding is also visible in the north-east of the domain, due to divergence of the rainfall area. The apparent contraction of the rain over north Wales (presumably due to orographic effects) leads to a false intensification of rain rate. Consequently, the area of rain over the Midlands is forecast to intensify when the radar shows it dying away.

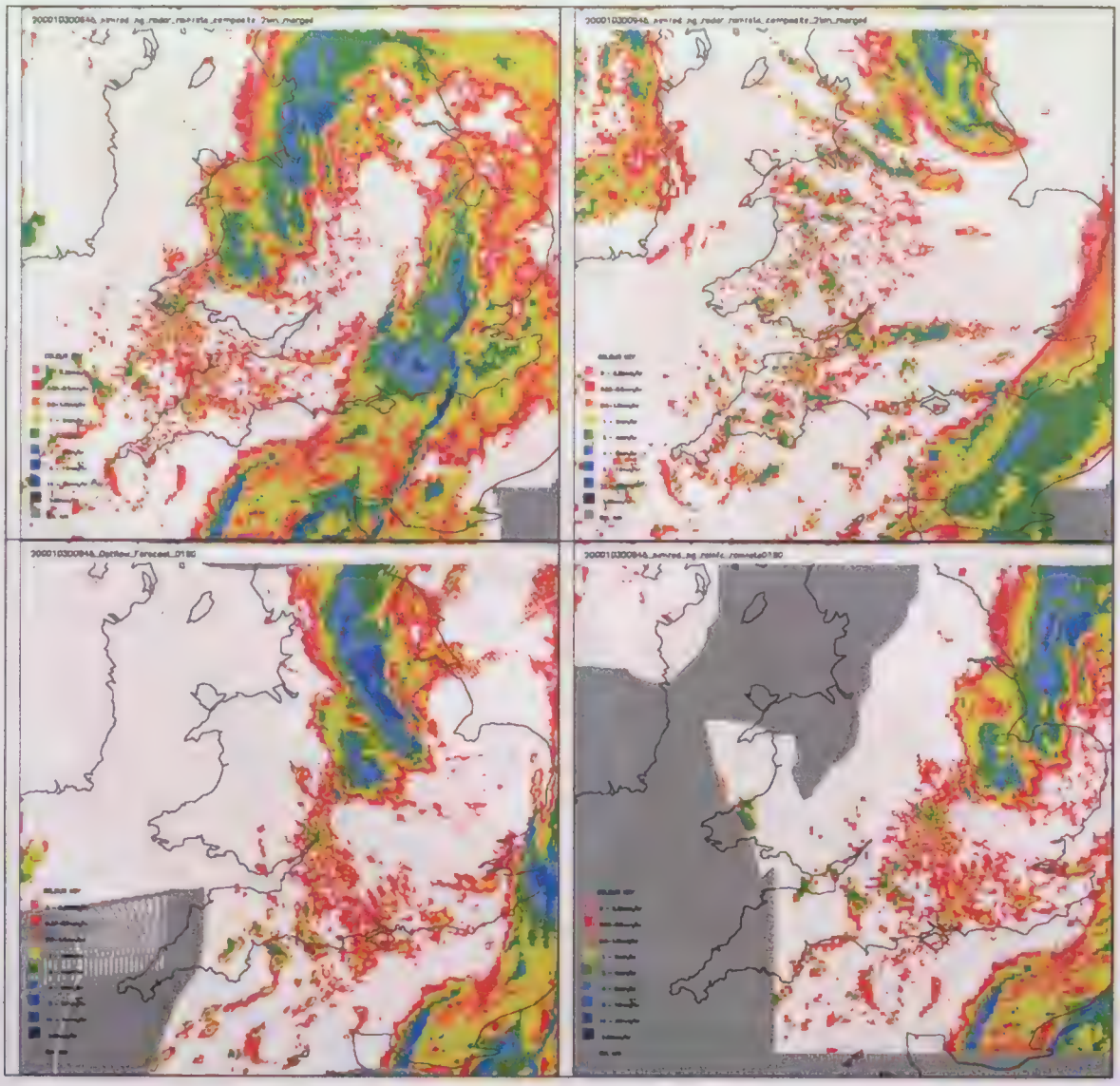

Figure 12. Verification of optic flow and Nimrod advection forecasts with a data time of 0645 GMT on 30 October 2000. The rain analyses valid at 0645 GMT (top-left) and 0945 GMT (top-right) should be compared with the T+3 hour forecasts from the optic flow (bottom-left) and Nimrod advection schemes (bottom-right).

4.1.4 3 April 2000

With a deep low pressure system in the Bay of Biscay, and high pressure to the north-west of Scotland, the UK lay under the influence of a strong surface pressure gradient oriented north-west to south-east. Aligned broadly with the surface isobaric pattern were a series of quasi-stationary fronts. Associated with these was a broad belt of rain aligned south-west to north-east across England and Wales. This almost stationary area of rain contained a number of small, more intense features evolving within it.

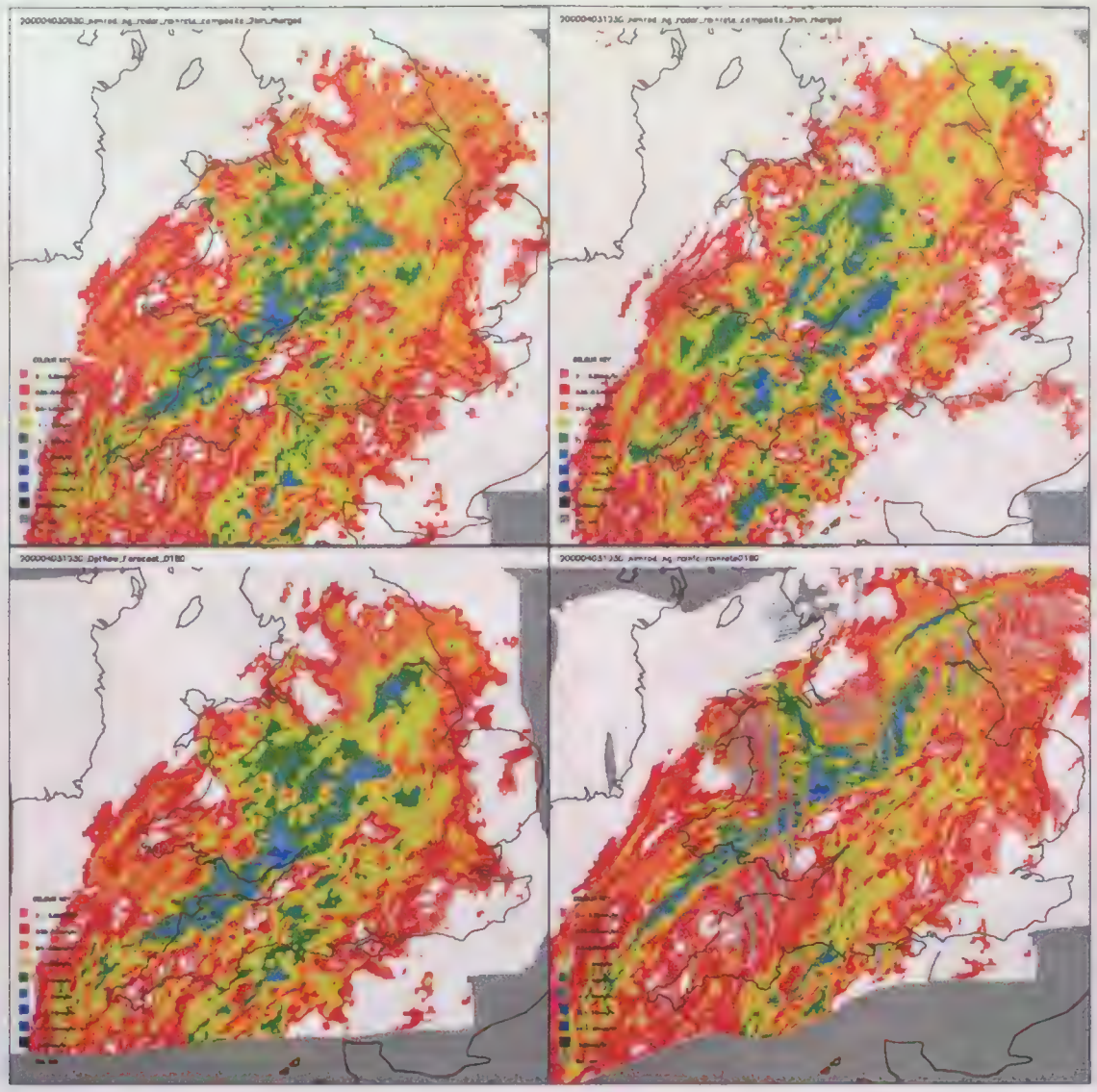

Figure 13. Verification of optic flow and Nimrod advection forecasts with a data time of 0930 GMT on 3 April 2000. The rain analyses valid at 0930 GMT (top-left) and 1230 GMT (top-right) should be compared with the T+3 hour forecasts from the optic flow (bottom-left) and Gandolf advection schemes (bottom-right).

On this occasion, the current Gandolf advection scheme (figure 13, bottom-right) used MM winds to produce the forecast. This captures the stationary nature of the rain band as a whole, but does produce noticeable and largely spurious motion within the band. As a result the fine scale detail in the forecast is inaccurate. Nonetheless, the verification statistics for Gandolf are competitive with the optic flow approach.

The advection velocities calculated by the optic flow scheme are much smaller, and the overall motion of the rain area is small. The intense area of rain over south Wales is not forecast to move. This is in agreement with the observed lack of motion in the verifying rain analysis (figure 13, top-right).

4.1.5 18 May 2000

Under the influence of low pressure to the north, the UK lay under the influence of several troughs. These produced widespread, showery rain as pictured in figure 14. The 0000 GMT ascent from Herstmonceux showed the troposphere to be unstable up to about 550 hPa. Although CAPE was limited, and no directional wind shear was observed, very little forcing was required to release this instability. Thus, showers were extensive but individual, convective cells were mostly short lived.

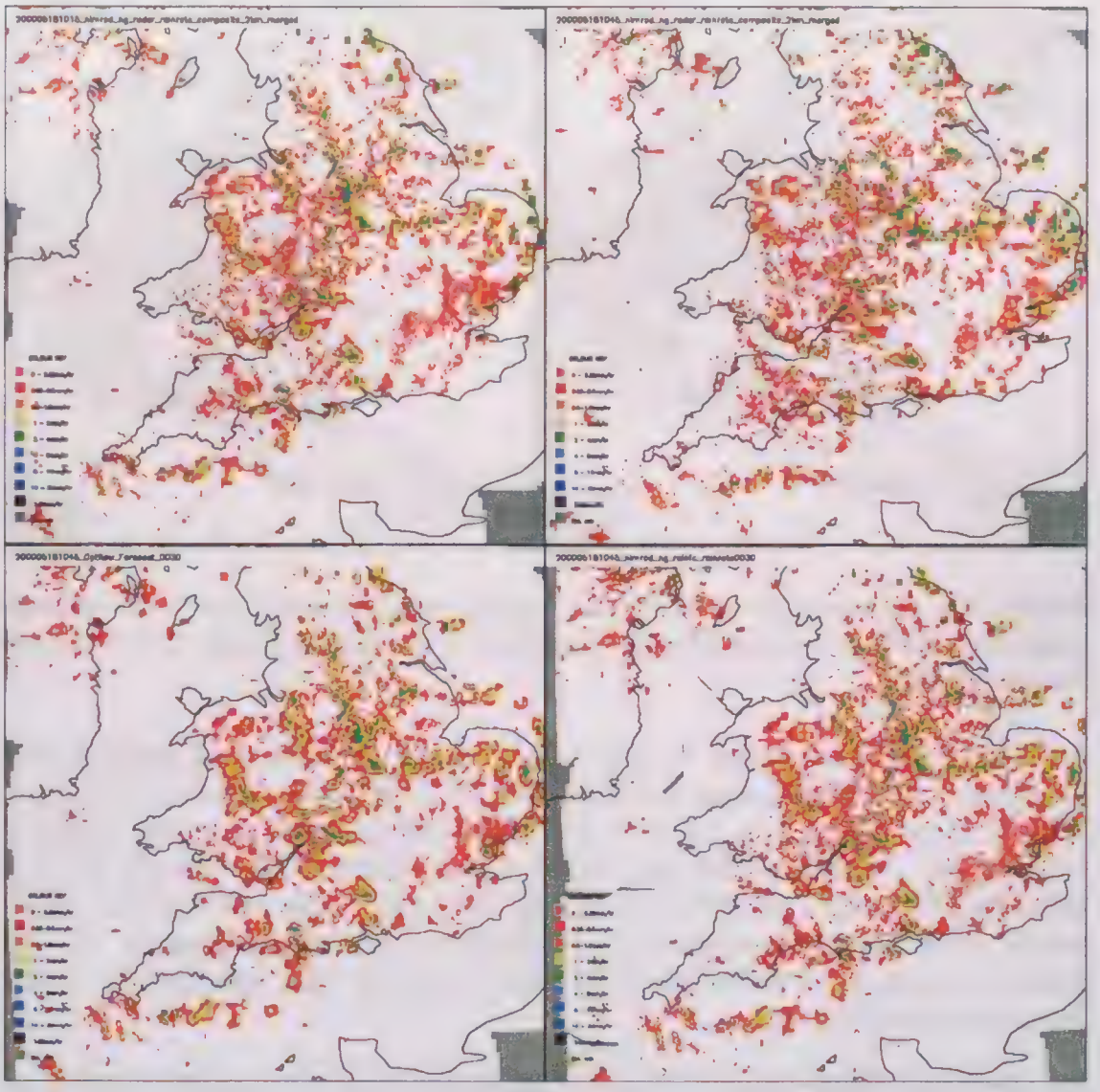

Figure 14. Verification of optic flow and Nimrod advection forecasts with a data time of 1015 GMT on 18 May 2000. The rain analyses valid at 1015 GMT (top-left) and 1045 GMT (top-right) should be compared with the T+30 minute forecasts from the optic flow (bottom-left) and Gandolf advection schemes (bottom-right).

Figure 14 demonstrates that both optic flow and Gandolf advection schemes have lost considerable accuracy in just 30 minutes. For example, a new area of rain was observed to develop over north Devon, but was not forecast by either scheme because the development of new rain areas is beyond the scope of extrapolation algorithms. Furthermore, Gandolf forecast the rain over Wales to move south and east, when, in reality, much of the rain remained stationary. The optic flow scheme scores better in this respect. On the other hand, the optic flow algorithm moves the rain away from the south coast of Devon too slowly. The timing of this departure is handled better by Gandolf.

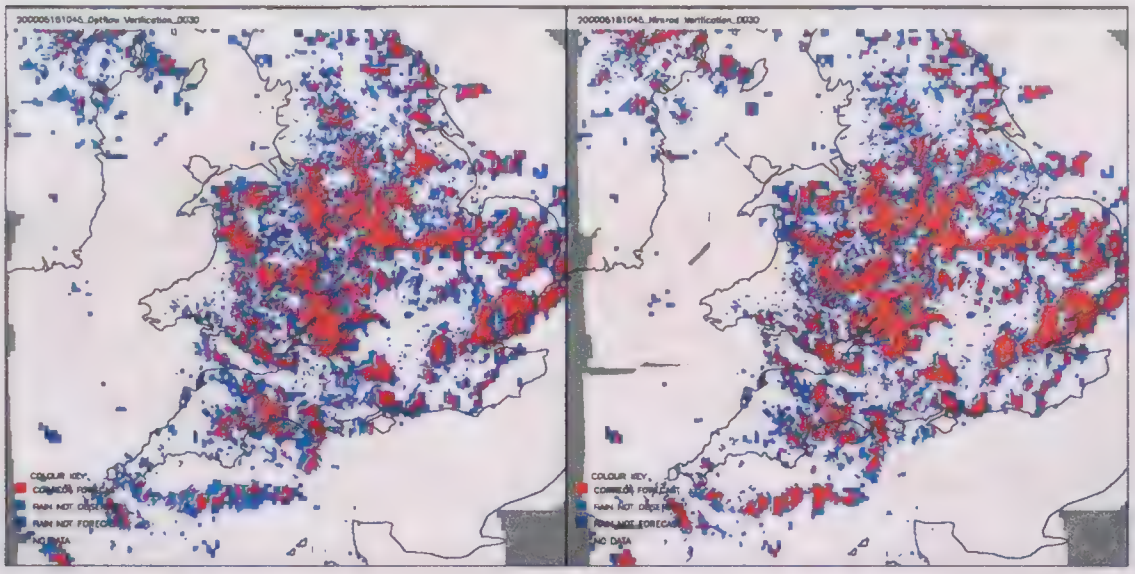

Figure 15. Categorical verification of predicted rain areas for T+30 minute optic flow (left) and Gandolf advection (right) forecasts valid at 1045 GMT on 18 May 2000.

A more informative picture of the relative quality of optic flow and Gandolf advection forecasts emerges by comparing forecast and observed rain areas. This is shown in figure 15, and indicates that Gandolf (hit rate 63%) is superior to optic flow (hit rate 52%) in this respect. The reason for this difference lies with Gandolf's use of MM wind advection. The use of a single model wind vector to advect each contiguous rain area (shower or shower cluster) produces a better forecast than methods that advect rain pixels separately (optic flow).

Of note is the finding that Gandolf's performance in terms of Hit Rate at T+30 minutes falls to 59% if linear extrapolation, as opposed to model wind advection, is used. One might conclude that MM winds are best for advecting showers, and that some benefit is to be gained from finding the best, single velocity for small precipitation areas. Perhaps this latter improvement could be incorporated into the optic flow scheme by changing r_n or the block size in accordance with the prevailing weather conditions.

4.1.6 21 February 2002

With low pressure systems located between Iceland and Scandinavia, the UK experienced broadly westerly winds. A series of fronts passed over the UK from the morning of 21 February 2002 onwards. The Herstmonceux ascent at 1200 GMT showed a small amount of static instability was confined to the lower troposphere, below the warm frontal surface. The precipitation associated with the front shown in figure 16 died away as it moved eastwards.

This is the type of case for which the current Gandolf advection scheme was developed – a broad band of rain moving across the UK. The optic flow scheme was not designed specifically for this type of scenario, but concern would be raised if it did not produce a creditable forecast.

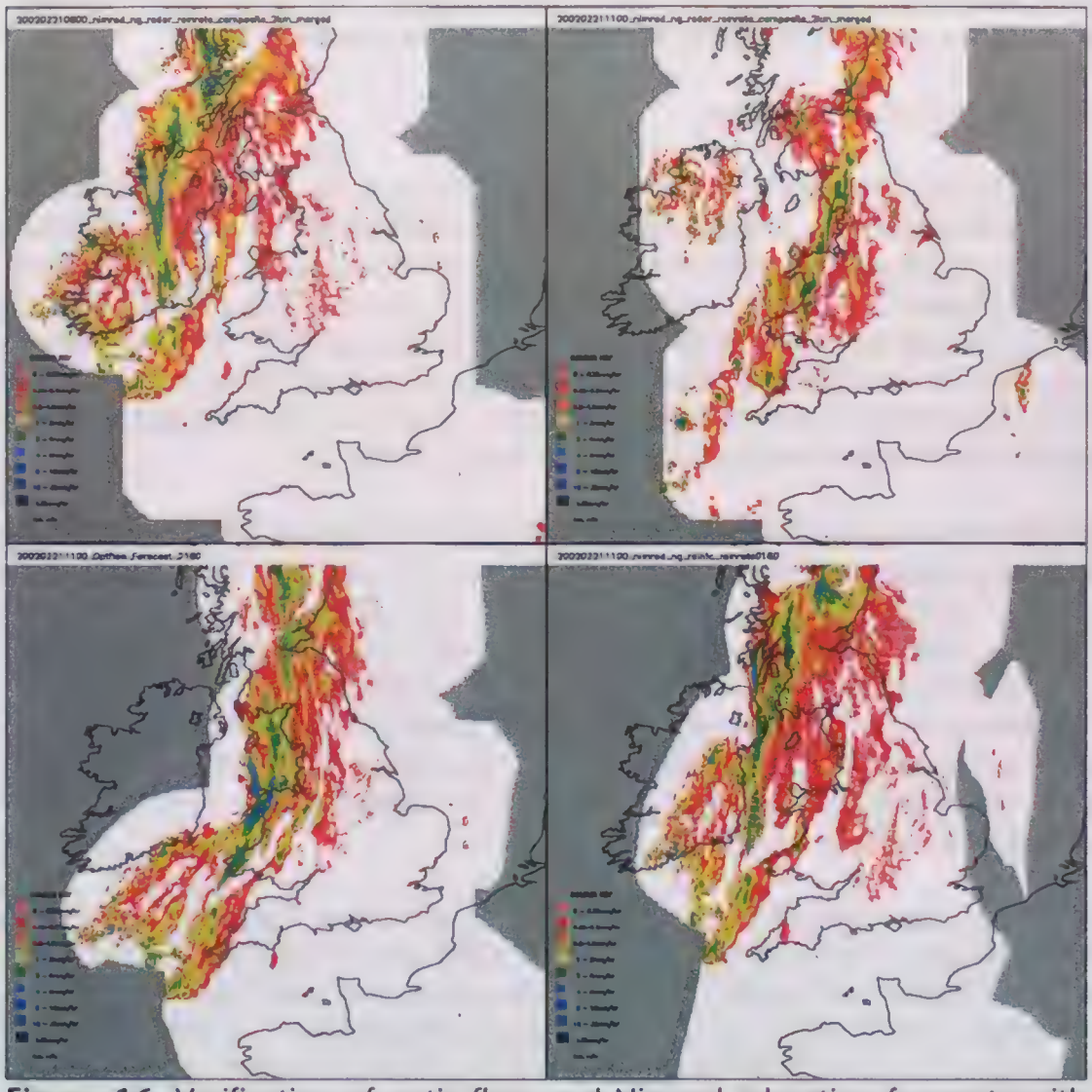

Figure 16. Verification of optic flow and Nimrod advection forecasts with a data time of 0800 GMT on 21 February 2002. The rain analyses valid at 0800 GMT (top-left) and 1100 GMT (top-right) should be compared with the T+3 hour forecasts from the optic flow (bottom-left) and Gandolf advection schemes (bottom-right).

The analysis pair on figure 16 show that the rain band changed in size and shape as it moved across the UK. The optic flow scheme allowed a contraction in the width of the frontal band, in reasonable agreement with the observed reduction in precipitation area. However, a portion of the rain area (over Anglesey) was forecast to intensify incorrectly. This intensification was a direct result of the contraction produced by the optic flow algorithm (total rain volume conserved). The area of rain over the Highlands of Scotland was not forecast to die away as observed.

Despite the limitations of the optic flow forecast, the Gandolf scheme performed less well in terms of rain–no-rain verification. Although it captured the motion of the frontal band with some accuracy, it was unable to change the predicted area of precipitation. As a result, the T+3 hour forecast in figure 16 demonstrates a large positive bias in this respect. On a more positive note the RMSE is comparable with that of the optic flow scheme.

4.2 Verification Statistics

The optic flow forecast scheme has been run once an hour using current Gandolf rain analyses as input. Optic flow forecasts (OPT) are compared with forecasts made using components of the Gandolf forecast scheme. These include advection forecasts produced by linear extrapolation advection (LEA) and MM wind advection (MWA), and a comparison with an unmodified version of the Gandolf advection scheme (ADV=LEA+MWA) [Pierce & Cooper, 2000]. The performance of each of these algorithms is assessed against baseline scores produced by Eulerian persistence (PER).

The performance statistics computed represent only a small selection of those commonly used to verify QPF performance (see [Forrester, 1999; Ebert and McBride, 1998]). They fall into two broad categories: continuous (RMSF [Forrester, 1999]) and categorical (CSI, HR, FAR). In the latter case, only the match between observed and forecast rain or no-rain areas is appraised; the magnitudes of the discrepancies between forecast and observed rain rates are ignored. It is important to recognise that these categorical statistics allow the merits of several forecasts to be assessed in relative rather than absolute terms, on an event by event basis.

The verification statistics considered here are those gathered between 1200 GMT on 7 February 2002 and 1100 GMT on 17 May 2002. At certain times the forecast schemes could not be run due to UNIX system stability problems, or because the rain analyses contained no rain. The statistics were gathered over a total of 2376 hours, with only 122 hours being missed during the verification period. One important point to note is that Gandolf (ADV) is not strictly comparable with optic flow (OPT) because the former integrates an orographic enhancement correction [Alpert & Shafir, 1989; Golding, 1998]. This gives the ADV a potential advantage in cases of orographically enhanced precipitation.

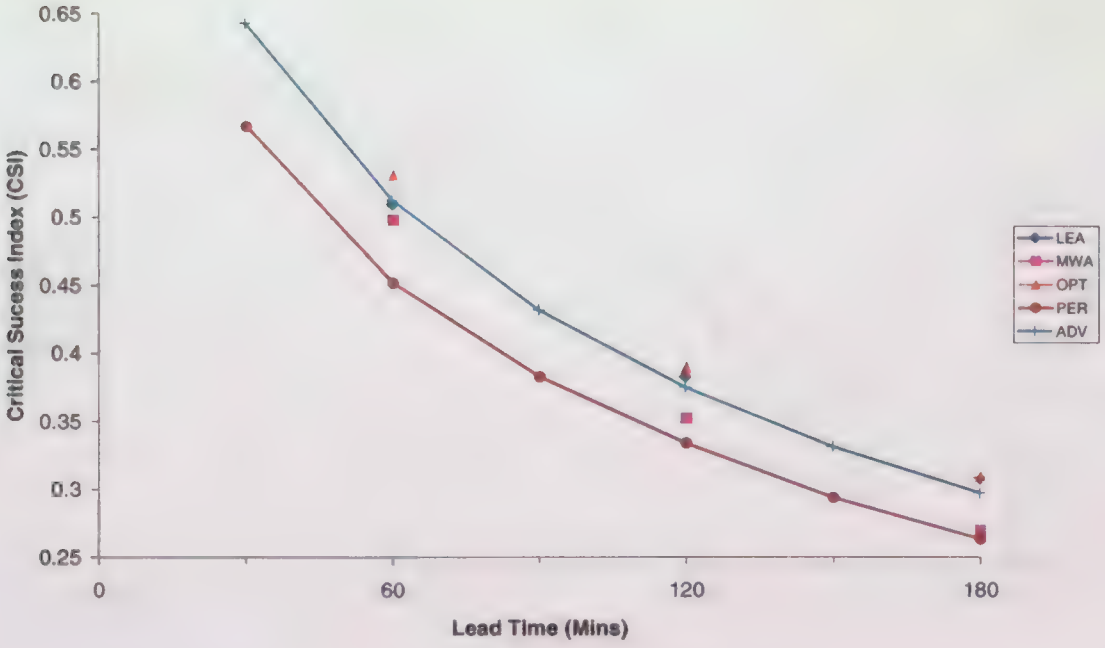

Figure 17. The relative performance of Gandolf advection (ADV), MM wind advection (MWA), linear extrapolation advection (LEA), optic flow (OPT) and Eulerian persistence (PER) forecasts as a function of lead time, as measured by the Critical Success Index (CSI). Statistics are averages over a 3 month period between 1200 GMT on 7 February 2002 and 1100 GMT on 17 May 2002.

Figure 17 compares the performance of the various forecast schemes using the Critical Success Index (CSI). Optic flow (OPT) is superior to the other schemes, including the current Gandolf advection scheme (ADV). MM wind advection (MWA) performs least well. Since Gandolf (ADV) is no better than linear extrapolation, the MM wind advection component of the Gandolf forecast scheme provides marginal benefit in terms of enhanced performance.

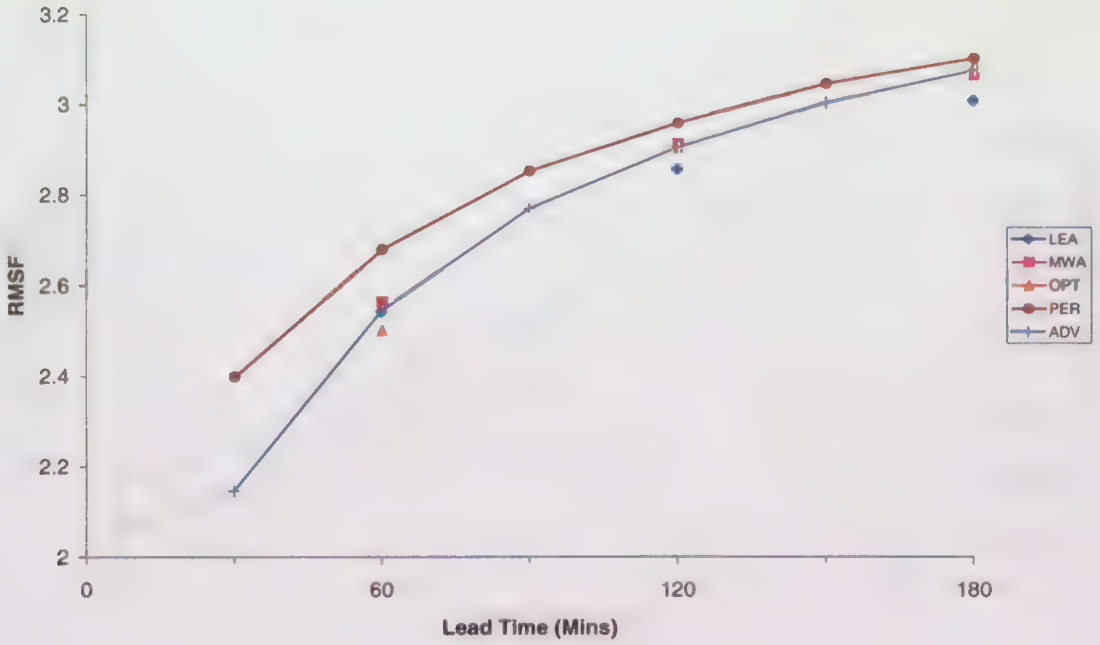

Figure 18. The relative performance of Gandolf advection (ADV), MM wind advection (MWA), linear extrapolation advection (LEA), optic flow (OPT) and Eulerian persistence (PER) forecasts as a function of lead time, as measured by the Root Mean Square Factor (RMSF). Statistics are averages over a 3 month period between 1200 GMT on 7 February 2002 and 1100 GMT on 17 May 2002.

Figure 18 presents the performance of the various forecast schemes in terms of the continuous statistic, Root Mean Square Factor (RMSF). In this case, optic flow (OPT) performs better than the other schemes for lead times of up to one hour. Thereafter, linear extrapolation (LEA) is superior. This finding is most likely attributable to the influence of the orographic enhancement algorithm which is not used by optic flow. At a lead time of 3 hours, linear extrapolation (LEA) clearly performs better than either the Gandolf advection scheme (ADV) or MM wind advection (MWA).

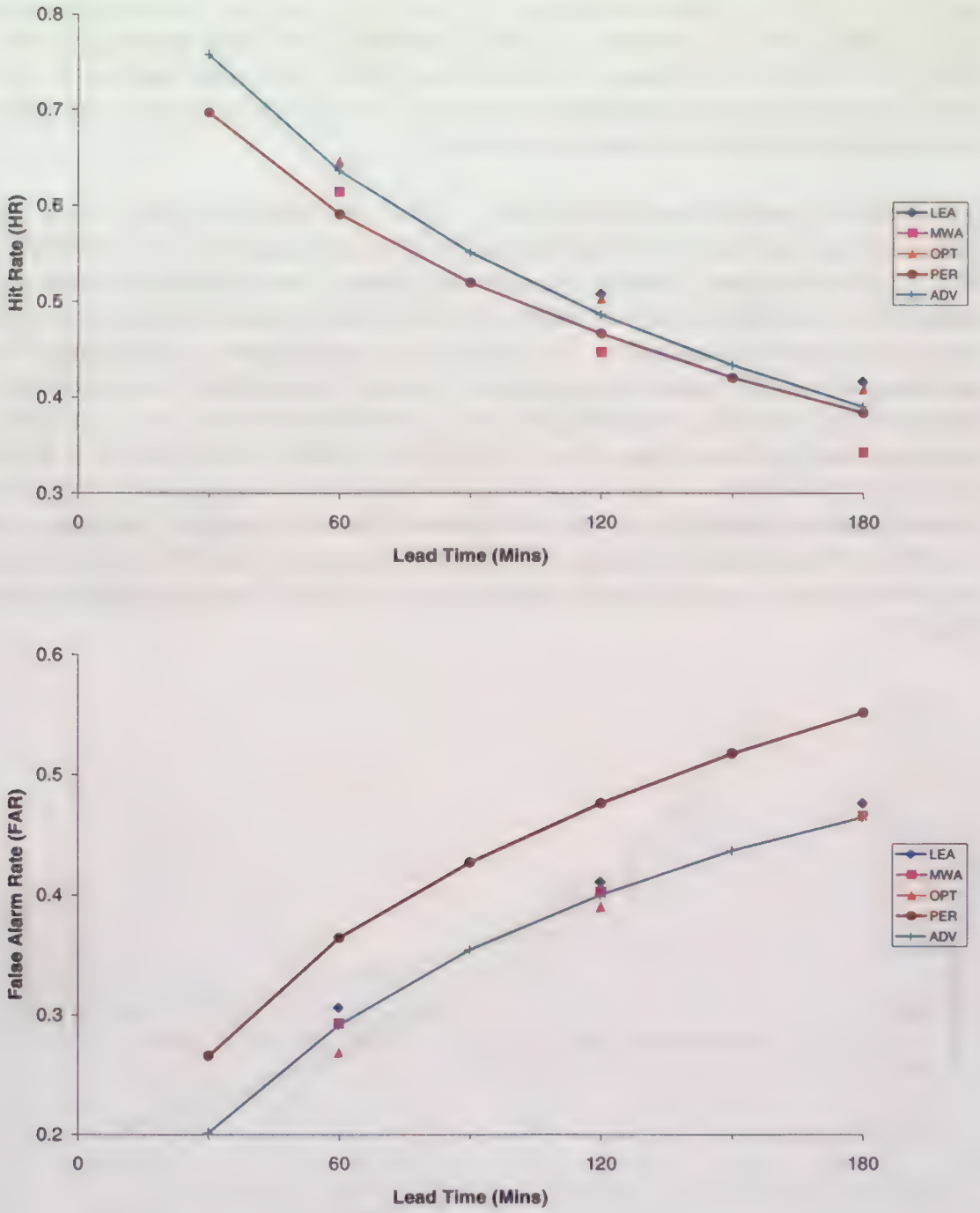

Figure 19. The relative performance of Gandolf advection (ADV), MM wind advection (MWA), linear extrapolation advection (LEA), optic flow (OPT) and Eulerian persistence (PER) forecasts as a function of lead time, as measured by the Hit Rate (HR) and False Alarm Rate (FAR). Statistics are averages over a 3 month period between 1200 GMT on 7 February 2002 and 1100 GMT on 17 May 2002.

Figure 19 expresses the performance of the various forecast schemes in terms of Hit Rate (HR) and False Alarm Rate (FAR). Linear extrapolation (LEA) is superior in terms of the HR, particularly at longer lead times. However, the performance of the optic flow scheme (OPT) is almost as good. MM wind

advection (MWA) performs poorly for HR, particularly at lead times of 2 hours and beyond, when it is inferior to persistence (PER). OPT has the lowest FAR. MWA has a better FAR than LEA at all lead times. This may be due to the advection of significant quantities of rain out of range of the composite radar network (and therefore the verification area).

Operational Gandolf forecasts blend a MM rain forecast (MM) with an extrapolation forecast (ADV), produced by a combination of LEA and MWA. This is likely to give Gandolf an advantage over pure advection schemes, especially at longer lead times when the effects of precipitation growth and decay can become important. To explore this issue, figure 20 compares the performance of the pure extrapolation schemes, LEA, MWA, with forecasts generated by merging these outputs with a MM rain forecast. The equivalent "merged" forecasts are referred to as LEM (LEA + MM), MWM (MWA + MM) and MGE (LEA + MWA + MM = Gandolf). Performance is expressed in terms of Critical Success Index (CSI). The results show that the "merged" products are superior to their advection only counterparts at longer lead times. However, the differences in performance between the merged schemes appear to be small.

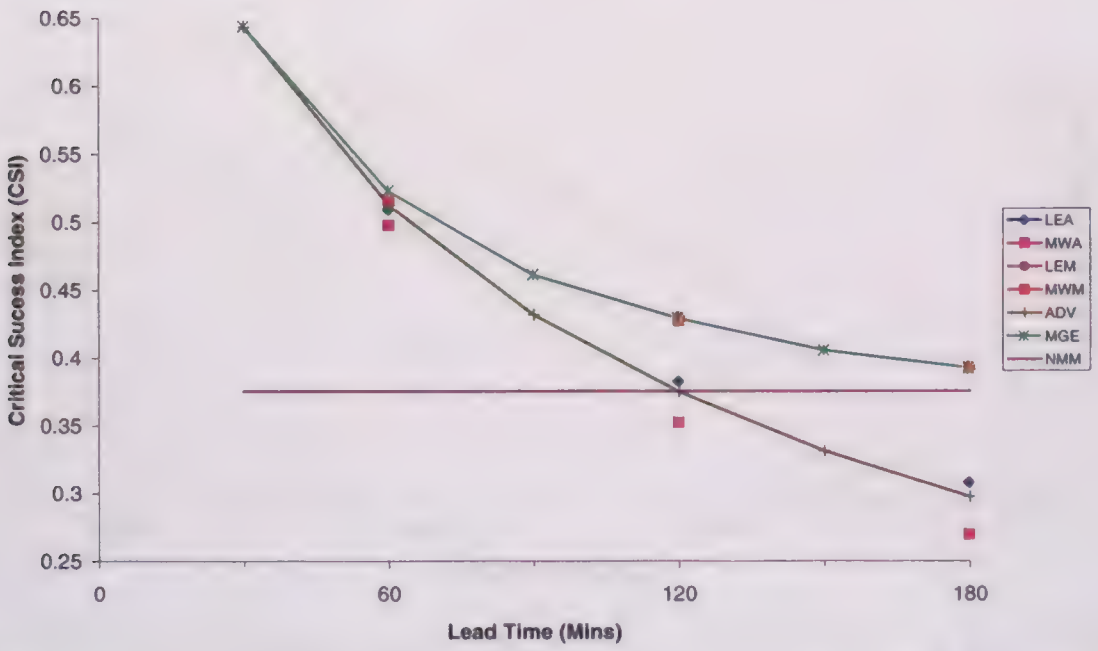

Figure 20. A comparison of the performance of the advection and "merged" versions of forecast schemes including Gandolf advection (ADV=LEA+MWA), Gandolf merged (MGE=LEA+MWA+MM), MM wind advection (MWA), MM wind merged (MWM=MWA+MM), linear extrapolation advection (LEA), and linear extrapolation merged (LEM=LEA+MM). Forecast performance, expressed in terms of Critical Success Index (CSI), is presented as a function of lead time. The statistics are averages over a 3 month period between 1200 GMT on 7 February 2002 and 1100 GMT on 17 May 2002.

5 Discussion

5.1 Embedded Convection

Although the optic flow advection scheme is not explicitly designed to cope with cases of embedded convection, it demonstrates a superior performance to the Gandolf advection scheme and its component algorithms (MWA, LEA) on such cases. Figures 15 and 16 show that the differential motion of the embedded convection is reproduced as faithfully as might be expected. The banding of the data behind the embedded feature is a product of the stretching applied to the forecast precipitation field in this area.

In principle, it might be possible to avoid this banding by using the continuity equation as a constraint (as in COTREC – [Li *et al.*, 1995]), as opposed to the smoothness condition (section 2.2). The affect of applying the former approach would be to produce a compensatory, backward flow of light rain to fill in the gaps left by the relative motion of the embedded convective rain. Clearly, optic flow does not handle embedded convection in an entirely satisfactory way. However, alternative approaches to the problem are subject to their own, no less significant flaws.

The application of a thresholding technique allows rainfall fields to be disaggregated on the basis of intensity. This affords an opportunity to apply different advection vectors to low and high intensity rain areas. This approach has been adopted in the Nimrod advection scheme. Whilst having the advantage of simplicity, such an approach is flawed because holes may appear in the resultant forecast rain field where high and low intensity components are advected with different velocities. Further more, it is not clear how the choice of threshold can be made in anything other than a rather arbitrary way.

A wavelet decomposition [Bruce & Gao, 1996] allows features in an image to be partitioned according to their size. A threshold on size may be used to separate embedded precipitation features from their "parent" objects. This naturally leads to the generation of negative rain rates. To avoid this effect, one may consider the features in a space of log (rain rate). This transformation introduces its own set of problems since the additive combination of features in log (rain rate) will make the total rain rate a product of the individual rain rates. Thus, total rain rate is not be conserved, and wild intensification of features may occur.

In summary, there are many possible approaches to the advection of embedded precipitation features. However, there is no clear “best” method that will reliably yield a good forecast.

5.2 Known flaws of the optic flow scheme

Successful application of the optic flow methodology depends critically upon estimation of the partial derivatives in the Optic Flow Constraint (OFC) equation. Rain objects that move across the boundary of a rain analysis within one time step cause a problem. In this case, $\frac{\partial I}{\partial t}$ is artificially large, and the estimated velocity can be in error. This is clearly demonstrated in the case study for 30 October 2000, when large differences are apparent in neighbouring velocities in the south-west corner of the rain analysis.

One solution to this problem involves ignoring blocks on the boundary of the rain analysis. Solution of the OFC is confined to the remaining blocks, and the velocities of boundary blocks are estimated using the smoothness constraint. This approach is flawed since these boundary velocities are not constrained to be realistic (see figure 16). As an alternative, one might consider using the MM as a constraint by imposing some maximum advection speed based upon MM wind forecasts. However, a simpler solution involves making use of additional rain observations outside the radar network (such as satellite rain and surface weather reports – see Wright, 1994), so that rain at the analysis boundaries is no longer important. The use of a temporal sequence of rain analyses to compute more stable block velocities is another alternative.

The false intensification or reduction of rain rate is evident in some optic flow forecasts (see for example figure 9). Observed increases in rain intensity are often accompanied by banding in the optic flow rain forecasts. Such banding is the product of diagnosed divergence in a rain analysis pair. This may happen when rain first appears in a portion of the latest rain analysis, either as a result of advection or new development. Conversely, observed decreases in rain intensity accompanying the decay of an area of rain may lead to the diagnosis of convergence by the OFC equation. The result is a false intensification of the rain.

The problems described above arise because the OFC makes explicit the assumption that rainfall does not change in intensity. Although this may be a good first approximation over short time intervals, it is quite clearly false when the temporal evolution of a rain field is rapid. Such is the case when a rain area is enhanced by travelling over elevated topography. For example, if an area of light rain intensifies as its leading edge meets higher ground, the spatial and temporal gradients of I increase. The result is a growth in the velocity estimation error.

One obvious solution to the orographic enhancement problem is to subtract the estimated, orographic component from the rain analysis before the optic flow scheme is applied. This can be added back afterwards, following the method currently adopted in Nimrod and Gandolf [Alpert and Shafir, 1989]. The rapid evolution of the precipitation field arising from meteorological

forcing is a more difficult issue to address. Recent studies have shown that the trending of rain intensity rarely improves forecast skill [Wilson *et al.*, 1998].

6 Conclusions and recommendation

A comparative trial of the optic flow forecast scheme with Gandolf and its component advection schemes, has shown the former to be superior in cases involving embedded convection, and differential precipitation motion. Despite these positive findings, there are certain aspects of the optic flow formulation, for example parameter estimation, that can be improved. These modifications can be expected to yield additional improvements in forecast quality.

Optic flow methods afford an additional, important advantage over the more traditional advection methods currently used by Nimrod and Gandolf. The OFC equation provides a sound basis for moving beyond the common assumption of Lagrangian persistence. The small differences in forecast performance exhibited by the optic flow and traditional advection schemes in this study suggest that there is little further improvement to be gained by working within this framework. Future advances in deterministic precipitation nowcasting are likely to come from modelling the evolution of rain intensity.

It is proposed that the optic flow forecast scheme replace the existing Nimrod advection scheme implemented in Gandolf. It should be integrated with the existing orographic enhancement algorithm, and the resultant forecasts should be merged with MM rain forecasts in a manner similar to that previously employed in the operational Gandolf system.

7 Recommendations For Further Work

Numerous aspects of the optic flow implementation described in this report remain to be improved. The more important of these are discussed below. Some of the proposed improvements can be expected to enhance forecast performance, but the magnitude of any single improvement is, on average, likely to be small.

The time interval between rain analysis pairs used in calculating the advection velocities may change the RMSE of a forecast by 10% (see figure 7). In the current version of the scheme the time step is 15 minutes, but this may not be optimal. The optimal choice of time step is likely to depend upon the prevailing weather conditions. This aspect of the implementation needs a thorough investigation. The use of a sequence of rain analyses to estimate advection velocities may prove more robust than a pair [Letang *et al.*, 1993, Nagel, 1995]. Such an approach would be suitable if five minute rain analyses become available.

The performance of the optic flow forecast scheme is dependent on the methods used to estimate the partial derivatives in the OFC equation. Currently, a simple method is employed, but more sophisticated techniques may bring a significant improvement in forecast skill. If such an improvement is forthcoming, there could be some additional benefits to be had from reducing the block size.

Allied to the above improvements is the use of alternative constraints on the deformation of the forecast rainfall field. The COTREC scheme successfully applies the continuity equation to the prediction of rainfall. The benefits of considering other constraints, such as divergence free motion, should be considered.

Estimation of the advection velocities at rain analysis boundaries remains a problem. One might consider combining the optic flow velocity field with a MM wind field. However, the motion of a precipitation fields is not always closely allied to that of the collocated wind field [Tatehira *et al.*, 1976; Browning & Collier, 1989]. Nonetheless, there may be some merit in using MM winds when precipitation is sparse.

The current method for apportioning rain from a single advected pixel between a set of pixels on the ground is simplistic and can lead to false intensification of rain areas. The method applied by Nimrod and Gandolf when using MM wind advection is more advanced and should be considered for future use.

8 References

Alpert, P., H. Shafir, (1989), "A physical model to complement rainfall normals over complex terrain", Journal of Hydrology, 110, 51-62

Bab-Hadiashar, A., D. Suter, (1998), "Robust optic flow computation", International Journal of Computer Vision, **29(1)**, 59-77

Browning, K. A., C. G. Collier, (1989) "Nowcasting of precipitation systems", Reviews of Geophysics, **27(3)**, 345-370

Bye P., M. Horner, (1998) "Easter 1998 Floods, Volume 1", Report by the independent review team to the board of the Environment Agency, P29

Bruce, A., H. Y. Gao, (1996) "Applied wavelet analysis with S-plus", Springer, New York; London

Forrester, D. A., (1999) "NWP verification system derivation of verification statistics", Met Office

Golding, B. W., (1998) "Nimrod: a system for generating automatic very-short-range forecasts", Meteorological Applications, 5, 1–16

Hand, W. H., (1996) "An object oriented technique for nowcasting heavy showers and thunderstorms", Meteorological Applications, **3**, 31-41

Horn, B. K. P., B. G. Schunck, (1981), "Determining optical flow", Artificial Intelligence, **17**, 185-203

Laroche, S., I. Zawadzki, (1995) "Retrievals of horizontal winds from single-Doppler clear-air data by methods of cross correlation and variational analysis", Journal of Atmospheric and Oceanic Technology, **12**, 721-738

Letang, J. M., V. Rebuffel, P. Bouthemy, (1993), "Motion detection robust to perturbations: a statistical regularization and temporal integration framework", 4th International Conference on Computer Vision, Berlin, 21-30

Li, L., W. Schmid, J. Joss, (1995), "Nowcasting of motion and growth of precipitation with radar over a complex orography", Journal of Applied Meteorology, **34**, 1286-1300

Nagel, H. H., (1995) "Optical flow estimation and the interaction between measurement errors at adjacent pixel positions", International Journal of Computer Vision, **15**, 271-288

NWP Index, http://www-cf/~cfver/nwpukpic/new5cpt36mnth.gif

O'Neil, P. V., (1995) "Advanced engineering mathematics (fourth edition)", PWS Publishing, 189-210

Pierce, C. E., A. M. Cooper, (2000) "Comparison of the performance of 2km resolution Object-Oriented Model and Nimrod advection precipitation nowcast schemes", Forecasting Research technical report No. 350, Met Office

Pierce, C. E., P. J. Hardaker, C. G. Collier, C. M. Haggett, (2000) "Gandolf: a system for generating automated nowcasts of convective precipitation", Meteorological Applications, **7**, 341-360

Tatehira, R., H. Sato, Y. Makino, (1976) "Short-term forecasting of digitised echo pattern", Kisho-cho Kenkyu Jiho, **28**, 61-70

Ulbrick, U., A. H. Fink, M. Klawa, J. G. Pinto, (2001) "Three extreme storms over Europe in December 1999", Weather, **56**, 76

Wilson, J. W., N. A. Crook, C. K. Mueller, J. Sun, M. Dixon, (1998), "Nowcasting thunderstorms: a status report", Bulletin of the American Meteorological Society, **79(10)**, 2079-2099

Wright, B., (1994), "A variational rainfall rate analysis scheme for Nimrod", Forecasting Research Division technical report No. 143, Met Office.